

Molecular recognition of genomic DNA in a condensate with a model surfactant for potential gene-delivery applications



Priya Singh^a, Susobhan Choudhury^a, Goutam Kumar Chandra^a, Peter Lemmens^{b,c}, Samir Kumar Pal^{a,*}

^a Department of Chemical, Biological & Macromolecular Sciences, S. N. Bose National Centre for Basic Sciences, Block JD, Sector III, Salt Lake, Kolkata 700 098, India

^b Institute for Condensed Matter Physics, TU Braunschweig, Mendelssohnstrasse 3, 38106 Braunschweig, Germany

^c Laboratory for Emerging Nanometrology, TU Braunschweig, Mendelssohnstrasse 3, 38106 Braunschweig, Germany

ARTICLE INFO

Article history:

Received 27 July 2015

Received in revised form 10 February 2016

Accepted 11 February 2016

Available online 12 February 2016

Keywords:

Molecular recognition

FRET

DNA condensate

Gene-delivery vehicle

Ultrafast dynamics

ABSTRACT

The functionality of a gene carrying nucleic acid in an artificial gene-delivery system is important for the overall efficiency of the vehicle *in vivo*. Here, we have studied a well-known artificial gene-delivery system, which is a condensate of calf thymus DNA (CT-DNA) with a model cationic surfactant cetyltrimethylammonium bromide (CTAB) to investigate the molecular recognition of the genomic DNA in the condensate. While dynamic light scattering (DLS) and circular dichroism (CD) reveal structural aspects of the condensate and the constituting DNA respectively, picosecond resolved polarization gated spectroscopy and Förster resonance energy transfer (FRET) reveal molecular recognition of the genomic DNA in the condensate. We have considered ethidium bromide (EB) and crystal violet (CV), which are well known DNA-binding agents through intercalative (specific) and electrostatic (non-specific) interactions, respectively, as model ligands for the molecular recognition studies. A fluorescent cationic surfactant, Nonyl Acridine Orange (NAO) is considered to be a mimic of CTAB in the condensate. The polarization gated fluorescence of NAO at various temperatures has been used to investigate the local microviscosity of the condensate. The excellent spectral overlap of NAO emission and the absorption spectra of both EB and CV allow us to investigate FRET-distances of the ligands with respect to NAO in the condensate at various temperatures and thermal stability of ligand-binding of the genomic DNA. The thermodynamic properties of the molecular recognition have also been explored using Van't Hoff equation. We have also extended our studies to molecular recognition of the genomic DNA in the condensate as dried thin films. This has important implications for its application in bioelectronics.

© 2016 Elsevier B.V. All rights reserved.

1. Introduction

The search for harmless synthetic vectors that allow an efficient delivery of genes for the treatment of genetic and acquired diseases leads to intense research activities and a wealth of literature in the last two decades [1–5]. Circumventing limitations associated with the viral vectors, e.g. packaging DNA with particular size, immunogenicity and mutagenicity, were the main motives of those studies. DNA condensates (complexes) with cationic surfactants/lipids are considered to be efficient candidates for gene-delivery (transfection) applications [6,7]. Among other obvious requirements for achieving efficient transfection, the most important factor is that the interaction of DNA with the vectors should yield a nanometer size close to that of viruses [4,8–10]. This requirement is closely related to the fact that the critical size limit for endocytosis is 150 nm and the condensate is expected to escape from the blood vessel if its size is beyond a limit [4,8]. Another important factor is the intactness of the duly hydrated B-form of the gene carrying DNA in the synthetic vector [5,11]. While the above important

considerations limit the efficiency of cationic polymers and cationic lipids, [12,13] cationic detergent cetyltrimethylammonium bromide (CTAB) is found to condense DNA into discrete particles containing even single nucleic acid molecule [14–16]. One of the notable properties of CTAB is the discrete first order phase transition of DNA between elongated coils and collapsed globules [15] well below the critical micellar concentration (CMC) of the surfactant and the formation of aggregates [15]. The interesting structure of the CTAB–DNA condensate is thought to result from the interaction of the negatively charged DNA phosphate groups with cationic surfactants and a further stabilization by the hydrophobic tails of the CTAB molecules [17].

Despite the unique feature of the CTAB–DNA condensate, the surfactant CTAB is found to be poorly efficient in transfection *in vitro* [18,19]. In order to study the sole role of CTAB in the stabilization of the CTAB–DNA condensate, in non-polar solvents rather than polar water media are the choice. The high solubility of the complex makes the contribution of parents (DNA and/or CTAB) inconclusive in the stability of the condensate in aqueous conditions. It was also concluded that due to higher solubility of the condensate, the complex in the cells is thought to induce fast release of CTAB revealing detergent related toxicity [4]. Earlier it has been shown that DNA-surfactant complexes are soluble

* Corresponding author.
E-mail address: skpal@bose.res.in (S.K. Pal).

in low-polarity organic solvents [3,20–22]. In one of these reports the structural properties of a genomic DNA upon complexation with CTAB in non-aqueous solvents of different degrees of polarity have been studied in details [3]. By using UV-vis, circular dichroism (CD) spectroscopy and fluorescence microscopy, the study has concluded that DNA–CTAB condensate dissociates into their initial components at concentrations of 40–60% (v/v) for ethanol or 30–50% (v/v) for 2-propanol, while conserving the double-stranded structure of the native DNA. Several other recent studies [23,24] unravel structural aspects of the genomic DNA in the condensate. However, the molecular recognition properties (both specific; intercalation, and non-specific; Coulombic) of the gene carrying DNA in the condensate are sparsely covered in the literature. In our earlier reports, the DNA-binding drugs Hoechst 33258 (non-specific) [25] and ethidium bromide (specific) [26] appear to be promising DNA-probes in the condensate. Ethidium bromide (EB) intercalates into the genomic DNA and provides the structural details of DNA even when it is in condensed form in a self-assembled micellar nanocage. On the other hand, Hoechst 33258, a well-known DNA minor groove binder, provides dynamical and structural information of the condensed DNA either bound to nucleic acid binding protein or CTAB surfactant [27]. It is important to note that the functional properties of gene carrying DNA (molecular recognition) in the condensate will dictate the overall activity of the gene after delivery in the target cells. A detailed investigation on the structural and functional properties (intercalation and electrostatic binding) of a genomic DNA (calf thymus; CT-DNA) in its condensate form in a non-aqueous solvent (butanol), where stabilization of the condensate is essentially governed by the hydrophobic tails of the CTAB surfactant, is the main motive of our present studies.

In the present work, we have synthesized a condensate of CT-DNA and CTAB in butanol. While dynamic light scattering (DLS) studies confirm the size of the condensate in the solution to be less than 100 nm, CD spectroscopy reveals the intactness of B-form structure of the genomic DNA in the condensate. Picosecond resolved fluorescence of a well-known DNA intercalator EB to the nucleic acid in the condensate clearly shows some degree of perturbation of the intercalative binding of the genomic DNA in the condensate compared to that in aqueous solution. We have measured the temperature dependent binding constant of the EB with the genomic DNA in the condensate in butanol and compared with that in aqueous solution. A detailed analysis of thermodynamical parameters from the Van't Hoff plots reveals that the EB-binding to the genomic DNA in the condensate is significantly different from that of the DNA in aqueous solution. In order to probe the interaction of CTAB in the condensate, we have used Nonyl Acridine Orange (NAO) as model cationic surfactant with a fluorescence acridine moiety [28,29]. Picosecond resolved polarization gated anisotropy of NAO in the condensate shows a hydrodynamic rotation of the surfactant in the condensate and reveals an activation energy for the viscous flow [30,31]. Strong spectral overlap of NAO emission and absorption spectrum of intercalating EB also offers the opportunity to measure the distance between cationic surfactant and the intercalator (EB) in the condensate with molecular precision employing Förster resonance energy transfer (FRET) strategy. We have also used FRET between NAO and another electrostatic DNA binder, crystal violet (CV) in the condensate. The constructed probability distribution functions of FRET distance between NAO and either EB (intercalator) or CV (electrostatic binder) at various temperatures in the condensate unravel the efficacy of molecular recognition of the genomic DNA by small ligands. Our studies are expected to find relevance in the investigation of functionality of DNA molecules in condensate for potential gene-delivery application.

2. Materials and Methods

2.1. Chemicals

Calf thymus DNA (CT-DNA), Nonyl Acridine Orange, ethidium bromide (EB) and crystal violet (CV) were purchased from sigma-Aldrich

(Saint Louis, USA) and were used as received. Cetyltrimethylammonium bromide (CTAB) and butanol were obtained from Spectrochem (Mumbai, INDIA) chemicals and Merck (Mumbai, INDIA), respectively. The aqueous solution of genomic DNA was prepared in phosphate buffer (50 mM, pH 7). In the present study the concentration of base-pair of the genomic DNA is considered as an overall concentration of DNA. The DNA concentration was determined by absorption spectroscopy, considering the molar extinction coefficient of DNA bases to be equal to $6600 \text{ M}^{-1} \text{ cm}^{-1}$ at 260 nm and found to be 6 mM [14].

2.2. Experimental Details

The steady state absorption and emission spectra were measured with Shimadzu UV-2600 spectrophotometer and Jobin Yvon fluorolog fluorimeter, respectively. CD spectra were recorded by JASCO-810 spectropolarimeter. Hydrodynamic diameter which were obtained from dynamic light scattering was measured by using Nano S Malvern instrument employing a 4 mW He-Ne laser ($\lambda = 632.8 \text{ nm}$) and equipped with a thermostated sample chamber. All the scattered photons were collected at a 173° scattering angle at $T = 298 \text{ K}$. The hydrodynamic diameter (d_h) of the particles is estimated from the intensity auto correlation function of the time-dependent-fluctuation in intensity. The diameter, d_h is define as, $d_h = \frac{k_B T}{3\pi\eta D}$, where k_B is the Boltzmann constant, T is the absolute temperature, η is the viscosity and D is the translation diffusion coefficient.

All the picosecond resolved fluorescence transients were measured by using commercially available time-correlated single-photon counting (TCSPC) setup with MCP-PMT from Edinburgh instrument, U.K. (instrument response function (IRF) of $\sim 90 \text{ ps}$) using a 409 nm excitation laser source. The sample temperature was maintained by a controller from Julabo (Model: F32). Details of the time resolved fluorescence setup have been depicted in our previous reports [25,32]. To estimate the FRET efficiency of energy donor (D) to the different acceptors (A) and hence to determine the distance of the FRET pair (D–A), we have followed the methodology described elsewhere [33–35]. In brief, D–A distance, r , can be calculated from the equation, $r^6 = [R_0^6(1 - E)]/E$, where E is the energy transfer efficiency between donor and acceptor, and R_0 is Förster distance.

For the fluorescence anisotropy measurements, the emission polarizer was adjusted to be parallel and perpendicular to that of the excitation and collected the fluorescence transients $I_{\text{para}}(t)$ and $I_{\text{perp}}(t)$, respectively. The anisotropy is defined as, $r(t) = \frac{(I_{\text{para}} - G \cdot I_{\text{perp}})}{(I_{\text{para}} + 2 \cdot G \cdot I_{\text{perp}})}$. The magnitude of G , the grating factor of emission monochromator of the TCSPC system, could be found using a long tail matching technique. The rotational relaxation time, τ_{rot} of the fluorescent probe is related to the local microviscosity, η_{lm} , experienced by the probe molecules through the Stokes–Einstein–Debye equation: [32] $\tau_{\text{rot}} = \eta_{\text{lm}} V_h / K_B T$ where K_B is the Boltzmann constant, T is the temperature, and V_h is the hydrodynamic volume of the probe.

Distance distribution function, $P(r)$ were calculated using nonlinear least-squares fitting procedure by using SCIENTIST software to the following function $P(r) = \{1/[\sigma - (2\pi)^{1/2}]\} \exp\{-1/2[(\bar{r} - r)/\sigma]^2\}$, where \bar{r} is the mean of the Gaussian with standard deviation of σ and r is the donor acceptor distance. Detailed theory and calculation of the distance distribution could be found elsewhere [36].

2.3. Preparation of DNA–CTAB Complex

The stock solution of the calf thymus DNA was diluted with the potassium phosphate buffer (50 mM, pH 7) so that the final concentration of the genomic DNA in nucleotide unit was 3 mM. To this solution, equimolar ratio of CTAB surfactant was mixed gently with continuous stirring. The resulting precipitate was separated and washed several times with the buffer solution. After that the precipitate was lyophilized

to prepare condensate powder. Similarly, four more samples were prepared following the above method: (a) DNA was precipitated with CTAB in presence of the cationic fluorescent surfactant NAO, (b) DNA labeled by EB was precipitated with CTAB, (c) DNA labeled by EB was precipitated with CTAB in presence of NAO and (d) DNA labeled with CV was precipitated with CTAB in presence of NAO. All complexes were dissolved in butanol for 6 to 7 h before the spectroscopic studies. DNA–CTAB thin film was prepared by uniformly spreading of solution on a quartz plate [37].

3. Results and Discussion

The normalized intensity distribution of scattered light from DLS on aqueous CTAB micelles and DNA are shown in Fig. 1(a). Hydrodynamic diameters for CTAB micelles (aqueous) and DNA (aqueous) are measured to be 4.8 nm and 187.0 nm, respectively, which are consistent with the reported literature [38–40]. However, the hydrodynamic diameter of CTAB in butanol is found to be 1.2 nm, which is the estimated length of the surfactant itself, indicating insignificant possibility of CTAB to form micelles in butanol. The diameter of the DNA–CTAB condensate is found to be 50 nm in butanol (Fig. 1(b)). During complexation the phosphate groups of DNA interact with the positive head group of CTAB resulting to a decrease in hydrodynamic diameter of the DNA–CTAB condensate. In order to understand structural perturbation of DNA due to its compactness in the condensate, we have performed CD spectroscopic studies. Fig. 1(c) shows the CD spectrum of the condensate in which the positive peak at 284 nm and negative peak at 253 nm are the signature of the B-form DNA in the condensate [23]. The structural integrity of the genomic DNA (B-form) in the condensate with respect to that in the aqueous buffer solution [27] is also clearly evident from the figure.

Upon confirmation of the structural integrity, functional properties (molecular recognition) of DNA in the condensate were investigated through intercalation of EB. Inset of Fig. 2(a) shows absorption and emission spectra of EB in DNA in aqueous solution and in the condensate. The absorption and emission maxima of EB in DNA in aqueous solution are at 518 nm and 595 nm, respectively, which are significantly red shifted to 539 nm and 616 nm, respectively, in the condensate indicating more polar environment in the vicinity of the probe in the genomic DNA upon complexation with CTAB [41]. Picosecond resolved fluorescence transients of EB in DNA (aqueous) and in condensate (butanol) are shown in Fig. 2(a). The bi-exponential fitting of the fluorescence decay of EB in DNA (aqueous) revealing ~22 ns as major component indicates that most of the EB is intercalated to the genomic DNA [26]. The shorter time constant (minor component) of ~1.8 ns is due to unbound EB in the aqueous solution [26]. The time constant is consistent with that of the free EB in aqueous solution revealing a ~1.6 ns component as shown in Fig. 2(b) and Table 1.

The fluorescence transient of the DNA-bound EB in the condensate shows triple exponential decay revealing typically time constants of ~1 ns (4%), 4.3 ns (21%) and 14 ns (75%). While the longer time constant (~14 ns) is the indicative of the DNA bound EB in the condensate, other two faster components indicate the population of loosely bound/free EB in the butanol solution. Our measurement of fluorescence transient of EB in bulk butanol reveals time constants of ~1 ns and 5 ns as shown in Fig. 2(b) and Table 1.

To gain insight into the thermal stability of the condensate, we have performed molecular recognition studies on the genomic DNA in the condensate at different temperatures. Upon increasing temperatures (10 °C to 60 °C) the relative percentage of the shorter components of EB–DNA fluorescence decays in aqueous solution and in the condensate are gradually increased. This observation is consistent with the fact that EB molecules are exposed towards the polar environments with increasing temperature. As evident from the insets of Fig. 3(a) the average lifetime for EB in the condensate is decreased from 11.9 ns at 10 °C to 8.2 ns at 60 °C, whereas average lifetime of EB in aqueous DNA is

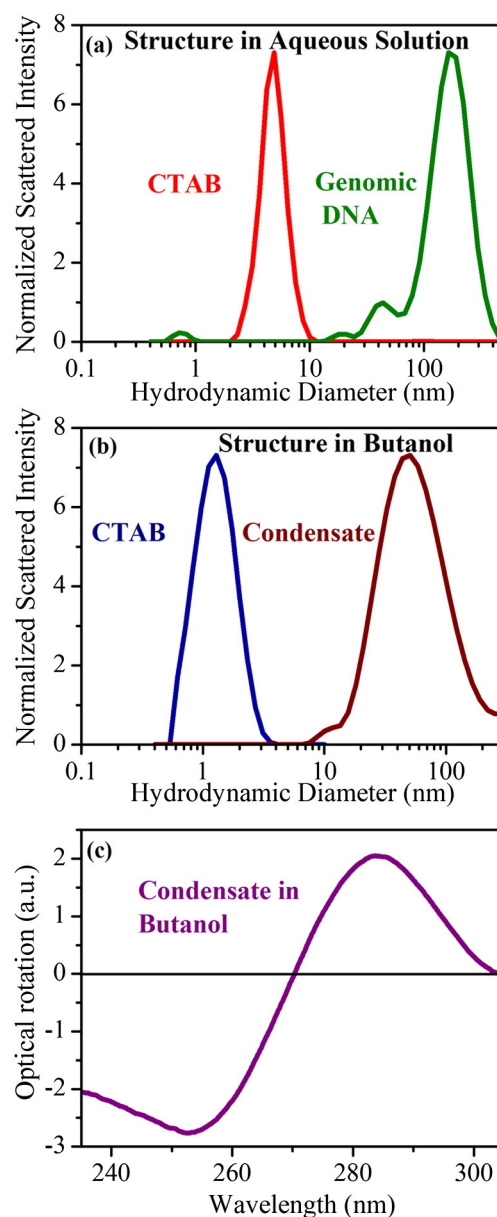


Fig. 1. Dynamic Light Scattering (DLS) of (a) CTAB micelle and DNA in aqueous solution (b) CTAB and the condensate (DNA–CTAB complex) in butanol. (c) CD spectra of DNA in condensate.

decreased from 22.0 ns at 10 °C to 19.2 ns at 60 °C (insets of Fig. 3(b)). We have estimated the binding constant K of EB with the genomic DNA and the condensate at different temperatures by using the following equation [26].

$$K = \frac{[EB-DNA]}{([EB] - [EB-DNA]) \times ([DNA] - [EB-DNA])} \quad (1)$$

where $[EB-DNA]$, $[EB]$ and $[DNA]$ represent the concentration of EB–DNA complexes, EB and the genomic DNA, respectively. The relative weighting of the longer and shorter components of EB fluorescence decays in the corresponding systems are indicative of bound and free population of the EB molecules, respectively. At room temperature, the binding constants of EB in two systems are found to be $470 \times 10^{-3} \mu\text{M}^{-1}$ (aqueous DNA) and $5.7 \times 10^{-3} \mu\text{M}^{-1}$ (condensate in butanol) indicating that EB binds to the DNA in aqueous solution more strongly than that in the condensate. The binding constant for the two systems were calculated at six different temperatures and

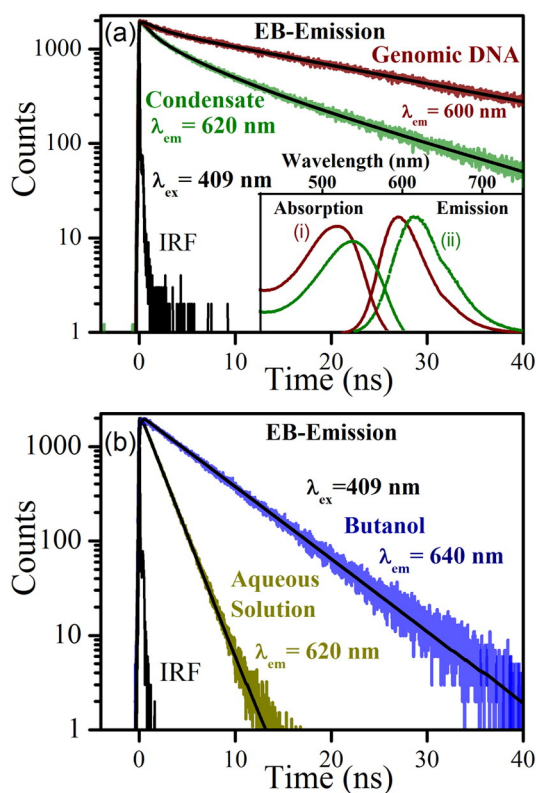


Fig. 2. (a) Picosecond resolved fluorescence transients of EB in DNA and in the condensate are shown. Inset shows the steady state spectra of EB in (i) DNA and (ii) the condensate. (b) Picosecond resolved fluorescence transients of EB in aqueous and in butanol are shown.

has been plotted against the inverse of temperature as shown in Fig. 3(a) and (b). The plotted data were fitted following the Van't Hoff equation [42,43].

$$\ln(K) = \frac{-\Delta H}{RT} + \frac{\Delta S}{R} \quad (2)$$

where R is the gas constant and T is the temperature in Kelvin. ΔH and ΔS were obtained from the slope and intercept of the linear Van't Hoff plot and ΔG can be obtained from the Gibbs Helmholtz equation [44].

$$\Delta G = \Delta H - T\Delta S = -RT \ln K. \quad (3)$$

The calculated value of ΔG , ΔH and ΔS is tabulated in Table 2. Negative values of both ΔG and ΔH for the two systems (genomic DNA and condensate) indicate that interactions are spontaneous and exothermic in nature. However, ΔS is found to be positive for DNA (aqueous) and negative for the condensate. Negative value of ΔH and positive value of ΔS in DNA (aqueous) indicate that EB binds through electrostatic interaction. For the condensate both ΔH and ΔS are negative, which corroborate that EB binds to the genomic DNA in the condensate through Van der Waals forces [45].

Table 1
The fluorescence life time of ethidium bromide (EB) in various systems.

system	τ_1 [ns] ([%])	τ_2 [ns] ([%])	τ_3 [ns] ([%])	τ_{avg} [ns]
DNA	1.8 (2.04)	22.0 (97.96)	0	21.6
Condensate	0.9 (3.75)	4.3 (21.13)	13.8 (75.11)	11.3
Aqueous	1.6 (100.0)	0	0	1.6
Butanol	0.9 (1.01)	5.5 (98.99)	0	5.4

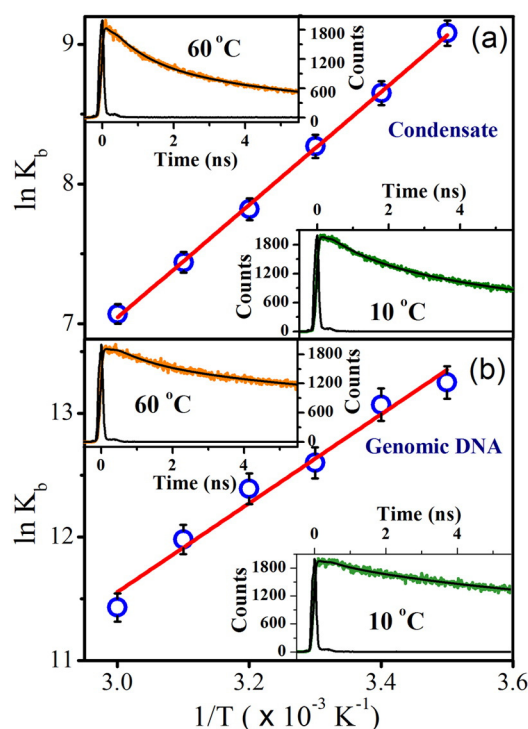


Fig. 3. The Van't Hoff plot of $\ln K$ vs. $1/T$ for binding of EB to (a) the condensate and to (b) DNA (with $\pm 1\%$ error bar for both the cases) and picosecond resolved fluorescence transient at 10 °C and 60 °C for EB in condensate and in the genomic DNA are shown in inset of panel (a) and (b).

In order to study DNA–CTAB interactions in the condensate from the view point of the cationic surfactant (CTAB), we have used a fluorescent cationic surfactant NAO (acridine orange 10-nonyl bromide), having an acridine head group and a long alkyl tail in the condensate [46]. Absorption and emission spectra of NAO in the condensate are shown in the inset of Fig. 4(a). Time resolved fluorescence transient of NAO in the condensate is shown in Fig. 4(a). The three exponential fitting of the decay reveals an average time constant of 2.6 ns, which is much longer than that of free NAO in butanol (data not shown), indicating that NAO is attached to the condensate. For further confirmation of the binding of NAO with the condensate, we have performed temperature dependent polarization-gated fluorescence anisotropy measurements. The anisotropy decays of NAO in the condensate at two temperatures (20 °C and 70 °C) are shown in the insets of Fig. 4(b). As evident from Fig. 4(b) the rotational time constant (τ_{rot}) becomes faster upon increasing the temperature. We have estimated the microviscosities at different temperatures for the corresponding systems, using hydrodynamic radius of the probe to be 6.8 Å and plotted with $1/T$ (K^{-1}) as shown in Fig. 4(c). A linear fit of the plot to the data provides an activation energy of 5.76 kcal/mol from the equation: [47] $\eta = \eta_0 \exp[E_n/(RT)]$, where E_n is the activation energy for the viscous flow. The estimated binding constant is consistent with the fact that NAO is electrostatically bound to the genomic DNA in the condensate [48].

To study the specific interaction of the genomic DNA in the condensate with cationic surfactant NAO, the nucleic acid was first labeled by the intercalator EB. Fig. 5(a) shows that emission spectrum of NAO broadly overlaps with absorption spectra of EB in the condensate

Table 2
Thermodynamic parameters for the binding of ethidium bromide to DNA and their condensate.

System	ΔH_{obs} (kcal mol ⁻¹)	ΔG_{obs} (kcal mol ⁻¹)	$T\Delta S_{obs}$ (kcal mol ⁻¹)
DNA	-6.69	-7.56	0.87
Condensate	-7.57	-5.05	-2.52

without EB and NAO, respectively, revealing EB and NAO to be a possible FRET pair. Fig. 5(b) shows that the fluorescence transient of NAO in the condensate is decreased by addition of EB due to efficient energy transfer from NAO (donor) to EB (acceptor) in the condensate. The efficiency of energy transfer is found to be 57%. At room temperature (20 °C), the estimated Förster distance (R_0) and donor–acceptor distance are found to be 35 Å and 33 Å, respectively. The observation indicates that donor and acceptor are in close proximity revealing strong interactions between DNA and the cationic surfactant (NAO) to form the condensate. In order to confirm that FRET is solely due to interaction of DNA (intercalated with EB) with the CTAB mimic NAO, a control experiment has been performed, where EB was added in aqueous solution of NAO in CTAB micelles. The inset of Fig. 5(a) shows that the emission of NAO in the CTAB micelles significantly overlaps with the absorption spectrum of EB in aqueous solution. However, the inset in Fig. 5(b) shows that fluorescence transient of NAO in CTAB micelles (aqueous) has no

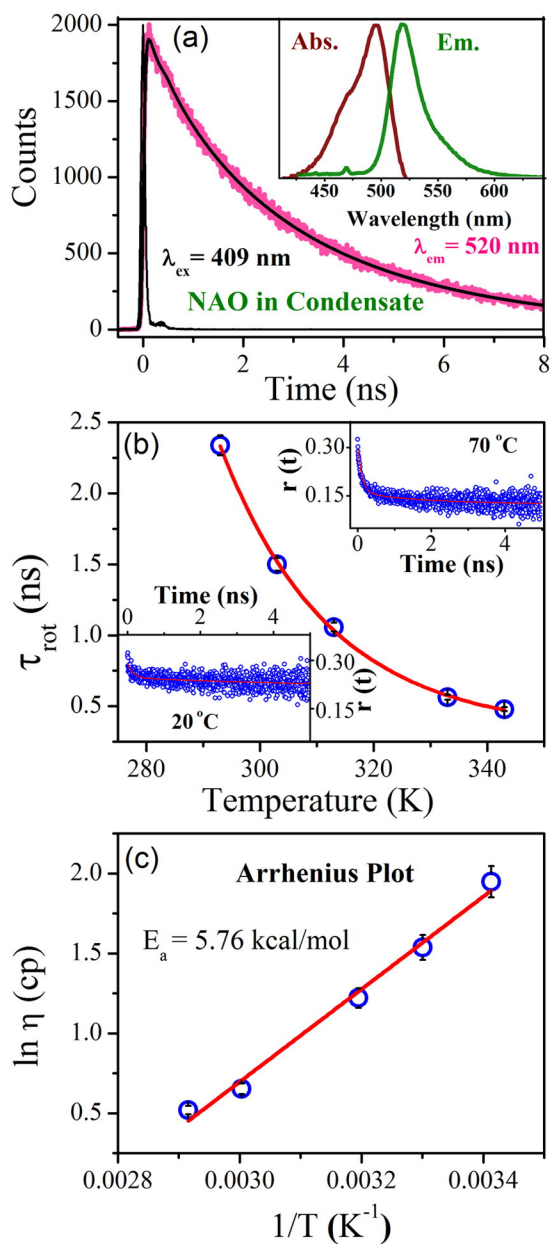


Fig. 4. (a) Picosecond resolved fluorescence transients of NAO in the condensate. Inset shows steady state spectra of NAO in condensate. (b) Plot of rotational time constants (τ_{rot}) against temperature for NAO in condensate (with $\pm 3\%$ error bar). (c) Arrhenius plot of microviscosities for NAO in condensate (with $\pm 5\%$ error bar).

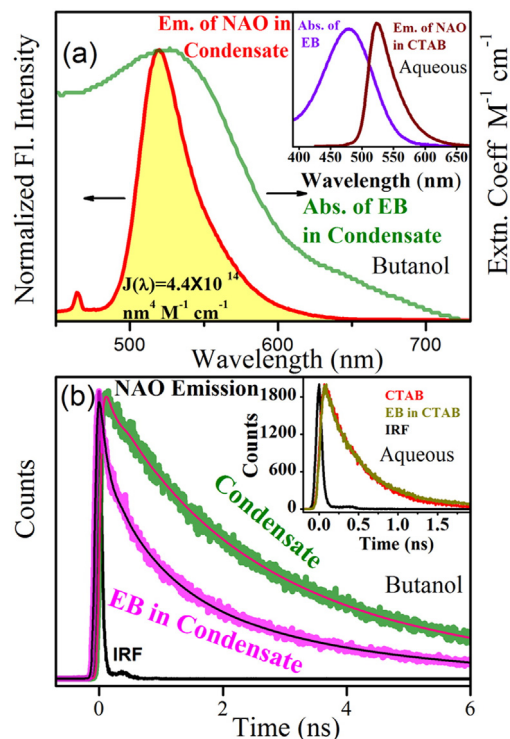


Fig. 5. (a) Spectral overlap of donor (NAO) and acceptor (EB) in condensate. Inset shows the spectral overlap of donor (NAO in CTAB micelles) and acceptor (EB) in aqueous solution. (b) Picosecond resolved transients of NAO in condensate in presence and absence of EB. Inset shows picosecond resolved transients of NAO in CTAB micelles in presence and absence of EB.

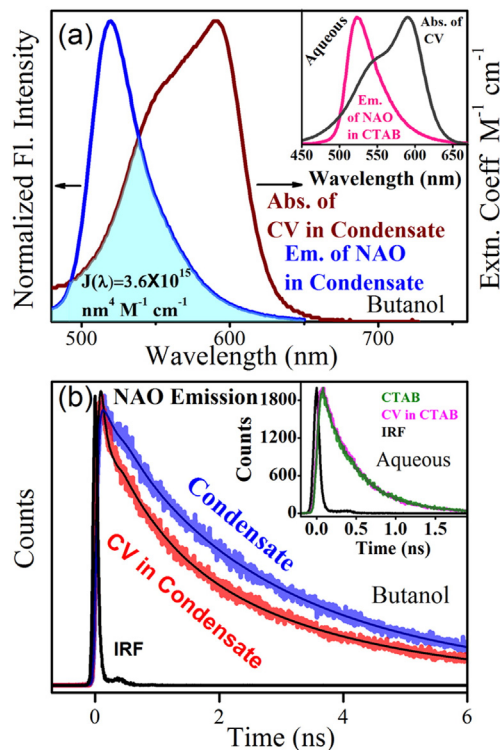


Fig. 6. (a) Spectral overlap of donor (NAO) and acceptor (CV) in condensate. Inset shows the spectral overlap of donor (NAO in CTAB micelles) and acceptor (CV) in aqueous solution. (b) Picosecond resolved transients of NAO in condensate in presence and absence of CV. Inset shows picosecond resolved transients of NAO in CTAB micelles in presence and absence of CV.

temporal quenching in presence of EB (without DNA), revealing that the quenching of fluorescence transients of NAO in the condensate is due to DNA-mediated energy transfer from NAO to EB. In presence of DNA, both positively charged CTAB and NAO are electrostatically bound to the nucleic acid and approach in the proximity of DNA-bound EB. However, the possibility of proximity of NAO to the energy acceptor EB in absence of DNA is completely absent (inset of Fig. 5(b)).

In order to study the nonspecific molecular recognition of a cationic dye (CV) by the genomic DNA in the condensate, we have performed the FRET studies to investigate the energy transfer from NAO to CV in the condensate. Fig. 6(a) shows that the emission spectrum of NAO overlaps (in condensate) with the absorption spectrum of CV (in the condensate). The fluorescence transient of NAO in the condensate is quenched in presence of CV as shown in Fig. 6(b). The efficiency of energy transfer in the above system is found to be 32%, which is lower than that in the case of EB as energy acceptor. The lower efficiency of energy transfer in non-specific interaction compared to that in the case of specific interaction (intercalation) may be due to higher mutual Coulombic repulsion of donor and acceptor having similar charges (cationic). The effect of the repulsion in the case of intercalated EB is lesser (Fig. 5b) than that of the loosely bound CV (Fig. 6(b)) [49]. The estimated Förster distance and donor (NAO)–acceptor (CV) distances are found to be 49 Å and 56 Å, respectively. Furthermore, in order to confirm that FRET is exclusively DNA-mediated, some control experiment has been done as shown in insets of Fig. 6(a) and (b) revealing no FRET in the absence of DNA in the micellar system in aqueous solution.

To study the fluctuation of the donor–acceptor distance we have performed picosecond resolved temperature dependent FRET study for the corresponding systems. Fig. 7(a) and the inset show temperature dependent FRET between NAO and EB in the condensate at 10 °C and at

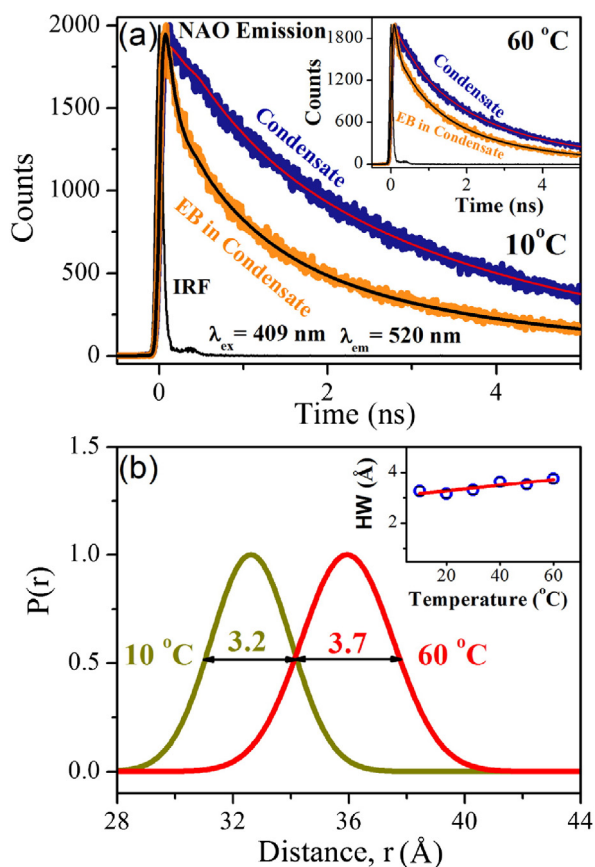


Fig. 7. (a) Picosecond resolved fluorescent transients of NAO in condensate in absence and presence of EB at 10 °C and at 60 °C are shown in inset, respectively. (b) Shows distribution of donor–acceptor distances of NAO and EB in condensate at 10 °C and at 60 °C. Inset shows plot of HW vs. temperature for the corresponding system (with $\pm 5\%$ error bar).

60 °C, respectively, clearly revealing that FRET efficiency is decreasing upon increasing temperature. The calculated donor–acceptor distance at the above two temperatures are found to be 33 Å and 36 Å, respectively. We have also calculated the distance distribution ($p(r)$) of donor–acceptor distance at different temperatures following the procedure reported earlier [35]. The distributions of NAO–EB distances in the condensate at temperatures 10 °C and 60 °C are shown in Fig. 7(b), which reveal that the distribution at lower temperature (half width, HW = 3.2 Å) is comparable to higher one (HW = 3.7 Å). The HW of the NAO–EB distances in the condensate is plotted against temperature yielding a linear thermal dependency of HW. With increasing temperatures, only distances between NAO and EB are found to be increased, however, the patterns of distributions (HW) of the distances are changed insignificantly (with experimental uncertainty of 5%) revealing the thermal stability, probably due to the fact that EB is strongly intercalated to DNA in the condensate.

Picosecond resolved temperature dependent FRET between CV and NAO in the condensate at 10 °C and at 60 °C are shown in Fig. 8(a) and in the inset, respectively. The FRET efficiency decreased significantly as compared to above system with increasing temperatures and the calculated donor–acceptor distances are found to be 53 Å and 64 Å at 10 °C and 60 °C, respectively. The distributions of donor–acceptor distances at the above temperatures are shown in Fig. 8(b), which reveal that the distribution at 60 °C (HW = 14.8 Å) is much broader than that of at 10 °C (HW = 5.5 Å). The plot of HW versus temperature provides the linear increment as shown in the inset of Fig. 8(b). The observation demonstrates that thermal fluctuations of the NAO–CV distances at higher temperatures increases in contrary to the earlier case of

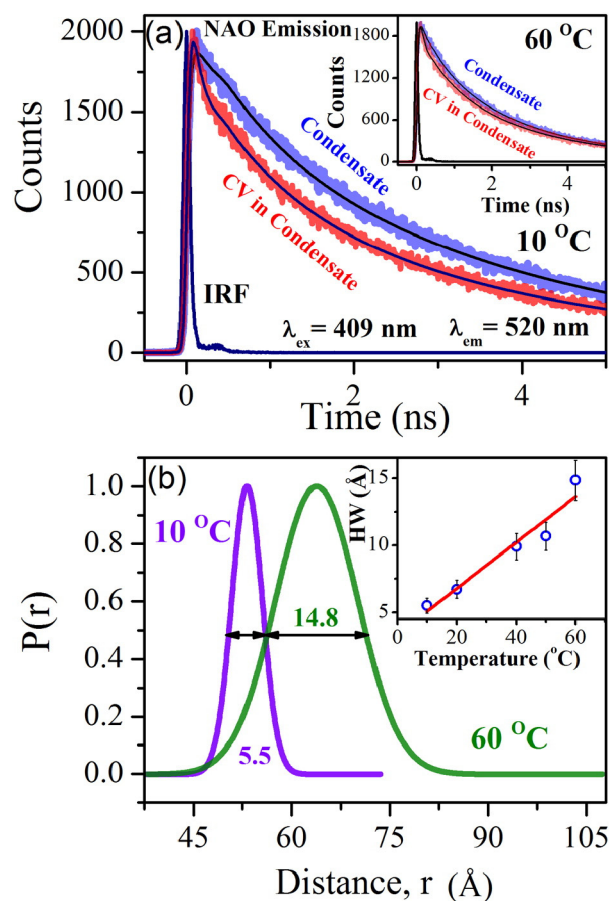


Fig. 8. (a) Picosecond resolved fluorescent transients of NAO in condensate in absence and presence of CV at 10 °C and at 60 °C are shown in inset. (b) Shows distribution of donor–acceptor distances of NAO and CV in condensate at 10 °C and at 60 °C. Inset shows a plot of HW vs. temperature for the corresponding system (with $\pm 10\%$ error bar).

NAO–EB system in the condensate [50]. It has to be noted that the fluctuation is not due to the instability of position of NAO in the DNA rather it is due to a relocation of CV at higher temperature. This is due to the fact that the observed insignificant fluctuation is present in the NAO–EB system, where EB was bound by intercalation to the genomic DNA in the condensate. As the condensate is found to be an attractive system for bioelectronics as thin films [51], we have also performed FRET studies on the efficacy of energy migration from NAO to DNA bound EB in the condensate as thin films. The efficient energy transfer from NAO to the acceptor EB is clearly evident from Fig. 9(a). Fig. 9(b) shows the distribution (HW = 2.7 Å) of donor–acceptor distance in thin film, which is lower than that of the solution phase may be due to the fact that in solid state the donor acceptor pair becomes less flexible.

4. Conclusion

In conclusion, we have performed a detailed study of an efficient gene-delivery system DNA–CTAB condensate. DLS experiments clearly show that DNA upon complexation with CTAB becomes compact in non-polar solvents. CD spectroscopy reveals that the B-structure of DNA remains unperturbed upon complexation with the CTAB surfactant. Using Van't Hoff equation, we have calculated binding constant of EB in DNA and the condensate at different temperature and found that EB binds strongly to DNA in compared to the condensate. The mode of binding of EB in DNA is electrostatic whereas in the condensate it binds through Van der Waals forces. We have also used polarization gated fluorescence anisotropy for the estimation of fluctuations of NAO in the condensate. From the microviscosities at different temperatures we have calculated the activation energy to be 5.76 kcal/mol for

the viscous flow, indicating electrostatic interactions with the genomic DNA in the condensate. In DNA–CTAB interaction we have found that FRET efficiency is higher when EB is used as acceptor instead of CV. The picosecond resolved temperature dependent FRET study for the corresponding system reveals that the distance between the donor and the acceptor increases significantly with increasing temperatures in case of CV compared to that of EB used as an acceptor. The fluctuation of donor acceptor distance is also higher in the case of a non-specific binding (CV) in comparison to specific binding (EB). Thus our findings are important to the future investigation on molecular recognition of DNA in the condensate and may find relevance in the design of an efficient gene-delivery agent.

Acknowledgments

SC thanks CSIR, India for the research fellowships. Financial grants (SB/S1/PC-011/2013) from DST (India) and (2013/37P/73/BRNS) from DAE (India) are gratefully acknowledged. PL thanks the NTH-School “Contacts in Nanosystem: Interaction, Control and Quantum Dynamics”, the Braunschweig International Graduate School of Metrology, and DFG-RTG 1953/1, Metrology for Complex Nanosystems.

References

- [1] I. Koltover, T. Salditt, J.O. Rädler, C.R. Safinya, An inverted hexagonal phase of cationic liposome–DNA complexes related to DNA release and delivery, *Science* 281 (1998) 78–81.
- [2] B. Pitard, O. Aguerre, M. Airiau, A.-M. Lachagès, T. Boukhnikachvili, G. Byk, C. Dubertret, C. Herviou, D. Scherman, J.-F. Mayaux, Virus-sized self-assembling lamellar complexes between plasmid DNA and cationic micelles promote gene transfer, *Proc. Natl. Acad. Sci. U. S. A.* 94 (1997) 14412–14417.
- [3] V.G. Sergeyev, S.V. Mikhailenko, O.A. Pyshkina, I.V. Yaminsky, K. Yoshikawa, How does alcohol dissolve the complex of DNA with a cationic surfactant? *J. Am. Chem. Soc.* 121 (1999) 1780–1785.
- [4] J. Clamme, S. Bernacchi, C. Vuilleumier, G. Duportail, Y. Mély, Gene transfer by cationic surfactants is essentially limited by the trapping of the surfactant/DNA complexes onto the cell membrane: a fluorescence investigation, *Biochim. Biophys. Acta Biomembr.* 1467 (2000) 347–361.
- [5] C.R. Safinya, K. Ewert, A. Ahmad, H.M. Evans, U. Raviv, D.J. Needleman, A.J. Lin, N.L. Slack, C. George, C.E. Samuel, Cationic liposome–DNA complexes: from liquid crystal science to gene delivery applications, *Phil. Trans. R. Soc. A* 364 (2006) 2573–2596.
- [6] J.P. Behr, Synthetic gene-transfer vectors, *Acc. Chem. Res.* 26 (1993) 274–278.
- [7] S. Satpathi, A. Sengupta, V. Hridya, K. Gavvala, R.K. Koninti, B. Roy, P. Hazra, A green solvent Induced DNA package, *Sci. Rep.* 5 (2015).
- [8] C. Watts, M. Marsh, Endocytosis: what goes in and how, *J. Cell Sci.* 103 (1992) 8.
- [9] D. Dey, C. Maiti, S. Maiti, D. Dhara, Interaction between calf thymus DNA and cationic bottle-brush copolymers: equilibrium and stopped-flow kinetic studies, *Phys. Chem. Chem. Phys.* 17 (2015) 2366–2377.
- [10] C.S. Braun, M.T. Fisher, D.A. Tomalia, G.S. Koe, J.G. Koe, C.R. Middaugh, A stopped-flow kinetic study of the assembly of nonviral gene delivery complexes, *Biophys. J.* 88 (2005) 4146–4158.
- [11] J.O. Rädler, I. Koltover, T. Salditt, C.R. Safinya, Structure of DNA–cationic liposome complexes: DNA intercalation in multilamellar membranes in distinct interhelical packing regimes, *Science* 275 (1997) 810–814.
- [12] D.D. Lasic, Liposomes within liposomes, *Nature* 387 (1997) 26–27.
- [13] J. Zabner, A.J. Fasbender, T. Moninger, K.A. Poellinger, M.J. Welsh, Cellular and molecular barriers to gene transfer by a cationic lipid, *J. Biol. Chem.* 270 (1995) 18997–19007.
- [14] M. Reichmann, S. Rice, C. Thomas, P. Doty, A further examination of the molecular weight and size of desoxyribose nucleic acid, *J. Am. Chem. Soc.* 76 (1954) 3047–3053.
- [15] S.M. Mel'nikov, V.G. Sergeyev, K. Yoshikawa, Transition of double-stranded DNA chains between random coil and compact globule states induced by cooperative binding of cationic surfactant, *J. Am. Chem. Soc.* 117 (1995) 9951–9956.
- [16] S.M. Mel'nikov, V.G. Sergeyev, Y.S. Mel'nikova, K. Yoshikawa, Folding of long DNA chains in the presence of distearyldimethylammonium bromide and unfolding induced by neutral liposomes, *J. Chem. Soc. Faraday Trans.* 93 (1997) 283–288.
- [17] S. Marchetti, G. Onori, C. Cametti, DNA condensation induced by cationic surfactant: a viscosimetry and dynamic light scattering study, *J. Phys. Chem. B* 109 (2005) 3676–3680.
- [18] P. Pinnaduwa, L. Schmitt, L. Huang, Use of a quaternary ammonium detergent in liposome mediated DNA transfection of mouse L-cells, *Biochim. Biophys. Acta Biomembr.* 985 (1989) 33–37.
- [19] J.K. Rose, L. Buonocore, M.A. Whitt, A new cationic liposome reagent mediating nearly quantitative transfection of animal cells, *Biotechniques* 10 (1991) 520–525.
- [20] V. Sergeev, O. Pyshkina, A. Zezin, V. Kabanov, DNA–surfactant complexes soluble in low-polarity organic liquids, *Polym. Sci. Ser. A Chem. Phys.* 39 (1997) 12–16.
- [21] K. Ijiro, Y. Okahata, A DNA–lipid complex soluble in organic solvents, *J. Chem. Soc. Chem. Commun.* (1992) 1339–1341.

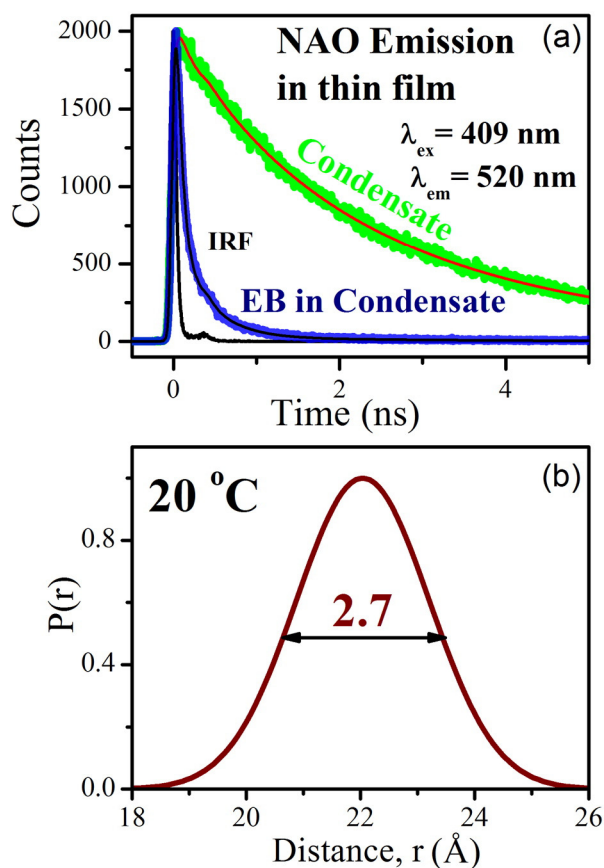


Fig. 9. (a) Picosecond resolved fluorescent transients of NAO in condensate in film form in absence and presence of EB. (b) Distribution of donor–acceptor distance of NAO and EB in condensate at room temperature (20 °C).

- [22] K. Tanaka, Y. Okahata, A DNA-lipid complex in organic media and formation of an aligned cast Film1, *J. Am. Chem. Soc.* 118 (1996) 10679–10683.
- [23] S. Marchetti, G. Onori, C. Cametti, Calorimetric and dynamic light-scattering investigation of cationic surfactant–DNA complexes, *J. Phys. Chem. B* 110 (2006) 24761–24765.
- [24] R. Marty, C.N. N'soukpoé-Kossi, D. Charbonneau, C.M. Weinert, L. Kreplak, H.-A. Tajmir-Riahi, Structural analysis of DNA complexation with cationic lipids, *Nucleic Acids Res.* 37 (2009) 849–857.
- [25] R. Sarkar, S.K. Pal, Interaction of Hoechst 33258 and ethidium with histone1–DNA condensates, *Biomacromolecules* 8 (2007) 3332–3339.
- [26] R. Sarkar, S.K. Pal, Ligand–DNA interaction in a nanocage of reverse micelle, *Biopolymers* 83 (2006) 675–686.
- [27] S. Choudhury, S. Batabyal, T. Mondol, D. Sao, P. Lemmens, S.K. Pal, Ultrafast dynamics of solvation and charge transfer in a DNA-based biomaterial, *Chem. Asian. J.* 9 (2014) 1395–1402.
- [28] T.H. Haines, N.A. Dencher, Cardiolipin: a proton trap for oxidative phosphorylation, *FEBS Lett.* 528 (2002) 35–39.
- [29] J.M. Petit, A. Maftah, M.H. Ratinaud, R. Julien, 10 N-nonyl acridine orange interacts with cardiolipin and allows the quantification of this phospholipid in isolated mitochondria, *Eur. J. Biochem.* 209 (1992) 267–273.
- [30] P.K. Verma, R.K. Mitra, S.K. Pal, A molecular picture of diffusion controlled reaction: role of microviscosity and hydration on hydrolysis of benzoyl chloride at a polymer hydration region, *Langmuir* 25 (2009) 11336–11343.
- [31] S. Patel, A. Datta, Fluorescence investigation of the binding of model PDT drugs to nonionic and zwitterionic surfactants, *Photochem. Photobiol.* 85 (2009) 725–732.
- [32] D. Banerjee, P.K. Verma, S.K. Pal, Temperature-dependent femtosecond-resolved hydration dynamics of water in aqueous guanidinium hydrochloride solution, *Photochem. Photobiol. Sci.* 8 (2009) 1441–1447.
- [33] J.R. Lakowicz, *Principles of Fluorescence Spectroscopy* Springer Science & Business Media 2013.
- [34] N. Polley, S. Singh, A. Giri, P.K. Mondal, P. Lemmens, S.K. Pal, Ultrafast FRET at fiber tips: potential applications in sensitive remote sensing of molecular interaction, *Sensors Actuators B Chem.* 210 (2015) 381–388.
- [35] S. Choudhury, P.K. Mondal, V.K. Sharma, S. Mitra, V.G. Sakai, R. Mukhopadhyay, S.K. Pal, Direct observation of coupling between structural fluctuation and ultrafast hydration dynamics of fluorescent probes in anionic micelles, *J. Phys. Chem. B* 119 (2015) 10849–10857.
- [36] S. Batabyal, T. Mondol, S. Choudhury, A. Mazumder, S.K. Pal, Ultrafast interfacial solvation dynamics in specific protein DNA recognition, *Biochimie* 95 (2013) 2168–2176.
- [37] L. Wang, J. Yoshida, N. Ogata, S. Sasaki, T. Kajiyama, Self-assembled supramolecular films derived from marine deoxyribonucleic acid (DNA)–cationic surfactant complexes: large-scale preparation and optical and thermal properties, *Chem. Mater.* 13 (2001) 1273–1281.
- [38] A.M. Wiosetek-Reske, S. Wysocki, Spectral studies of N-nonyl acridine orange in anionic, cationic and neutral surfactants, *Spectrochim. Acta A* 64 (2006) 1118–1124.
- [39] M. Cárdenas, K. Schillén, T. Nylander, J. Jansson, B. Lindman, DNA compaction by cationic surfactant in solution and at polystyrene particle solution interfaces: a dynamic light scattering study, *Phys. Chem. Chem. Phys.* 6 (2004) 1603–1607.
- [40] T. Movchan, I. Soboleva, E. Plotnikova, A. Shchekin, A. Rusanov, Dynamic light scattering study of cetyltrimethylammonium bromide aqueous solutions, *Colloid J.* 74 (2012) 239–247.
- [41] R. Bera, B.K. Sahoo, K.S. Ghosh, S. Dasgupta, Studies on the interaction of isoxazolcurcumin with calf thymus DNA, *Int. J. Biol. Macromol.* 42 (2008) 14–21.
- [42] G. Zhang, X. Hu, P. Fu, Spectroscopic studies on the interaction between carbaryl and calf thymus DNA with the use of ethidium bromide as a fluorescence probe, *J. Photochem. Photobiol. B* 108 (2012) 53–61.
- [43] N. Akbay, Z. Seferoğlu, E. Gök, Fluorescence interaction and determination of calf thymus DNA with two ethidium derivatives, *J. Fluoresc.* 19 (2009) 1045–1051.
- [44] R.K. Nanda, N. Sarkar, R. Banerjee, Probing the interaction of ellagic acid with human serum albumin: a fluorescence spectroscopic study, *J. Photochem. Photobiol. A* 192 (2007) 152–158.
- [45] P.D. Ross, S. Subramanian, Thermodynamics of protein association reactions: forces contributing to stability, *Biochemistry* 20 (1981) 3096–3102.
- [46] E. Mileykovskaya, W. Dowhan, R.L. Birke, D. Zheng, L. Lutterodt, T.H. Haines, Cardiolipin binds nonyl acridine orange by aggregating the dye at exposed hydrophobic domains on bilayer surfaces, *FEBS Lett.* 507 (2001) 187–190.
- [47] R.K. Mitra, P.K. Verma, S.K. Pal, Exploration of the dynamical evolution and the associated energetics of water nanoclusters formed in a hydrophobic solvent, *J. Phys. Chem. B* 113 (2009) 4744–4750.
- [48] M. Eftink, C. Ghiron, Dynamics of a protein matrix revealed by fluorescence quenching, *Proc. Natl. Acad. Sci. U. S. A.* 72 (1975) 3290–3294.
- [49] W. Müller, F. Gautier, Interactions of heteroaromatic compounds with nucleic acids. A–T-specific non-intercalating DNA ligands, *Eur. J. Biochem.* 54 (1975) 385–394.
- [50] S. Nag, B. Sarkar, M. Chandrakesan, R. Abhyankar, D. Bhowmik, M. Kombrabail, S. Dandekar, E. Lerner, E. Haas, S. Maiti, A folding transition underlies the emergence of membrane affinity in amyloid- β , *Phys. Chem. Chem. Phys.* 15 (2013) 19129–19133.
- [51] A.J. Steckl, DNA—a new material for photonics? *Nat. Photonics* 1 (2007) 3–5.